PROPERTIES AND POTENTIAL FOR APPLICATION OF STEEL REINFORCED POLYMER (SRP) AND STEEL REINFORCED GROUT (SRG) COMPOSITES

X. Huang[1], V. Birman[2], A. Nanni[1], and G. Tunis[3]
[1] Civil Engineering, University of Missouri – Rolla, Rolla, MO 65409
[2] Engineering Education Center in St. Louis, University of Missouri – Rolla, St. Louis, MO 63121
[3] Hardwire, LLC, Pocomoke City, MD 21851

The paper introduces steel reinforced polymer (SRP) and steel reinforced grout (SRG) composites that are considered for application in civil engineering for bridge and concrete buildings upgrade. These composites consist of steel cords formed by interwoven steel wires embedded within a polymer resin or cementitious grout matrix. The properties of SRP are evaluated experimentally and compared to micromechanical equations to determine a suitability of these equations for the prediction of material constants. The effectiveness of SRP is evaluated on existing structures (i.e., slab strips of a parking garage) while SRG performance is studied on laboratory-prepared large-scale reinforced concrete beams. It is shown that both composites significantly enhance the strength of the concrete members providing the first evidence of their suitability for practical applications concerned with upgrading the existing infrastructure. Improvements subsequent to the testing to both the cord design and fabric manufacturing process show even greater promise.

SRP composites consist of steel wires forming cords that are assembled into a fabric and embedded within a polymeric matrix. A cross section of such cord photographed under a microscope is depicted in Fig. 1. Performance of a composite material utilizing steel wires is controlled by the stress transfer between the wires and the matrix. A single high-strength wire may be deficient due to low interfacial shear strength and stiffness. This problem is solved in SRP by using twisted steel filaments forming the cord, as shown in Figs. 2. The rough surface of the cord provides mechanical interlock with the matrix resulting in a system suitable for structural applications. As an example, the cord shown in Fig. 2 is produced by twisting one wire at a short lay length around 12 wires that are twisted in a long lay length. The warp wire provides additional surface roughness and tightens the cord enhancing its integrity. Steel cords employed in the present study had a diameter equal to 0.044 in and consisted of 13 filaments. Several different impregnating resins were considered, including Epon 828 + Hardener HT-386, M-Brace Saturant, SikaDur 330 and SikaTop 121. Epon 828 was used in the tests described in this paper.

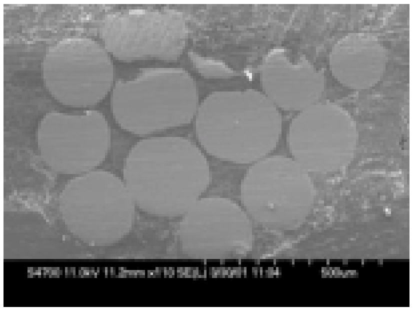

Fig. 1.

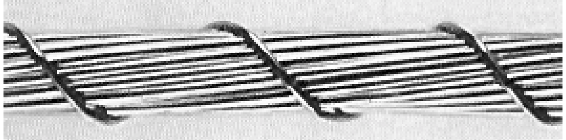

Fig. 2.

Unidirectional SRP samples were tested in tension and compression using an MTS 880 testing machine. The specimens were premanufactured using compression molding into a plate, shipped to the laboratory, and cut to size by waterjet. The volume fraction of steel wires in the composite material was equal to 0.27.

Experiments were conducted on a large number of specimens. The average experimental values of engineering constants of SRP are presented in Table 1. This table also presents the values predicted by the improved mechanics of materials micromechanical theory. As follows from the table, theoretical predictions for the tensile and compressive longitudinal modulus of elasticity and for the in-plane shear modulus are in good agreement with experimental data. The agreement for tensile transverse modulus of elasticity and for both Poisson ratios is less satisfactory. Nevertheless, even these material constants can be adequately predicted by the micromechanical theory considered in the paper. However, the compressive modulus could not be obtained from micromechanics.

Table 1

	Experimental	Analytical	
$E_1(ksi)$ Ten.	8159	8397	
$E_1(ksi)$ Comp.	11400	11826	
$E_2(ksi)$ Ten.	849	910	
$E_2(ksi)$ Comp.	1240	914	
ν_{12} Ten.	0.395	0.342	
ν_{12} Comp.	0.380	0.342	
ν_{21} Ten.	0.047	0.041	
ν_{21} Comp.	0.032	0.026	
$G_{12}(ksi)$	320	336	

The main application of SRP is envisioned in the situations where these composites are subject to longitudinal tension. Accordingly, it is also important to compare the longitudinal strengths available from the experiments (122 ksi) to the theoretically predicted value. The latter value is obtained by the rule of mixtures and it is equal to 126 ksi that is remarkably close to the experimental result. This strength can be further improved by increasing the packing density of the cords (available with the new manufacturing process) and by moving to one of the higher property cords.

The flexural strength of SRP was evaluated from a three-point bending test designed according to ASTM D 790. Detailed description of the tests is omitted since it can be found in this standard. A typical load-midspan deflection curve for one of the specimens is shown in Fig. 3. The modes of failure were rupture on the tensile surface of the specimens and fiber microbuckling on their compressed surface. The effect of these modes of failure, particularly fiber microbuckling and related softening of the response, is clearly observed in Fig. 3. The average flexural strength of SRP found in these tests was equal to 101.1 ksi.

Four strips were cut out of the deck of a parking garage in Clayton, Missouri and they were reinforced by plies of FRP (carbon/epoxy) and SRP. Both FRP and SRP reinforcements increased the ultimate capacity of the beams by over 100%. This illustrates the potential of SRP in repair and retrofitting of concrete elements of infrastructure.

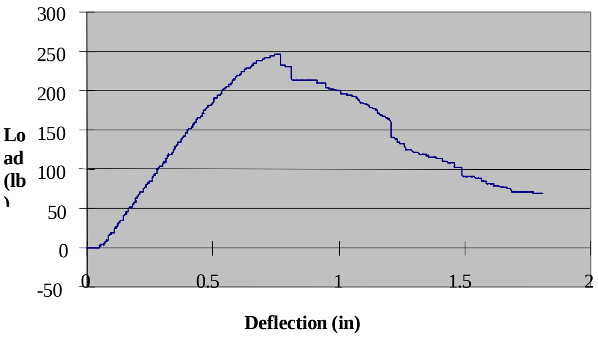

Fig. 3.

SRG represents an alternative to SRP where a resin matrix material is replaced with cementitious grout. The feasibility of SRG strengthening for concrete beams was experimentally investigated by comparing the performance of three reinforced concrete beams subject to four-point bending.

The load-midspan deflection relationships for three beams are shown in Fig. 4. The load and deflection corresponding to the initiation of cracking in concrete are clearly observed for all three beams. Prior to cracking, the beams have an almost identical stiffness. The increases in the yield stress for SRP and SRG over the yield stress of the control beam were 33% and 7%, respectively. The ultimate loads of the beams were 67 kips (SRP), 62 kips (SRG), and 51 kips (control beam). The ultimate failure occurred at midspan of the beams. The failure was brittle and controlled by peeling of the strengthening. Based on experimental results, it is apparent that SRG, even thought less effective than SRP, has good potential in structural applications.

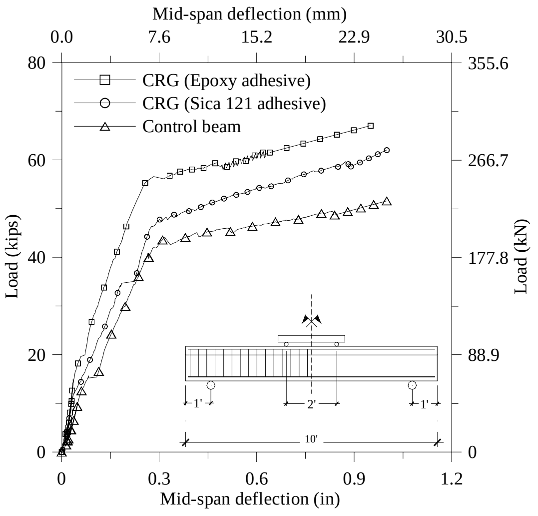

Fig. 4.

In conclusion, it has been shown that SRP and SRG represent promising materials for strengthening of concrete structures. The properties of these materials can be predicted by micromechanical theory. Low cost and ease of manufacture of SRP and SRG strengthening elements further contribute to their attractiveness in applications.